GEOMECHANICS RESEARCH SERIES 3

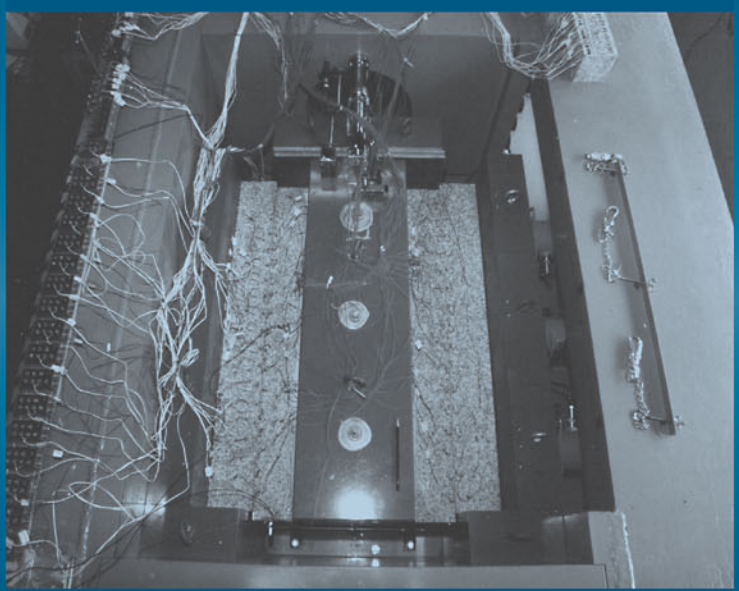

EXPERIMENTAL ROCK MECHANICS

KIYOO MOGI

EXPERIMENTAL ROCK MECHANICS

BALKEMA – Proceedings and Monographs
in Engineering, Water and Earth Sciences

Experimental Rock Mechanics

Kiyoo Mogi
Emeritus Professor of the University of Tokyo

Taylor & Francis
Taylor & Francis Group
LONDON / LEIDEN / NEW YORK / PHILADELPHIA / SINGAPORE

Taylor & Francis is an imprint of the Taylor & Francis Group, an informa business

This edition published in the Taylor & Francis e-Library, 2006.

"To purchase your own copy of this or any of Taylor & Francis or Routledge's collection of thousands of eBooks please go to www.eBookstore.tandf.co.uk."

Published by: Taylor & Francis/Balkema
P.O. Box 447, 2300 AK Leiden, The Netherlands
e-mail: Pub.NL@tandf.co.uk
www.balkema.nl, www.taylorandfrancis.co.uk, www.crcpress.com

British Library Cataloguing in Publication Data
A catalogue record for this book is available from the British Library

Library of Congress Cataloging-in-Publication Data
Mogi, Kiyoo, 1929–
Experimental rock mechanics/Kiyoo Mogi.
p. cm.

Includes bibliographical references.
ISBN 0–415–39443–0 (hardcover : alk. paper) 1. Rock mechanics. I. Title.

TA706.M64 2006
624.1'5132—dc22

2006004322

ISBN 0-203-96444-6 Master e-book ISBN

ISBN 10: 0 415 39443 0 (Print Edition)
ISBN 13: 978 0 415 39443 7
ISSN: 0929-4856

Table of contents

Preface

This book does not aim to cover every problem of rock mechanics in a systematic manner. Rather, it touches upon selected subjects of a fundamental character and, in particular those pertinent to tectonophysics and seismology. Furthermore, it does not attempt to review all the developments but concentrates on my own contribution to the field of experimental rock mechanics. As a geophysicist, and a seismologist in particular, I have had an interest in the fracture and flow of rocks under stresses since the very beginning of my scientific career. In the field of seismology, I have written a book "Earthquake Prediction" (Academic Press, Tokyo, 1985). In parallel to these researches, I have pursuied experimental studies of the mechanical behaviour of rocks in the laboratory since about 1960.

In this book I will present, in detail, experimental methods developed and results obtained over the years by myself and my co-workers mainly at the Earthquake Research Institute of the University of Tokyo. In particular, many pages will be devoted to the problem of the deformation and fracture of rock specimens under the general triaxial compression in which all three principal stresses are different. Although this is one of the most fundamental and important problems, there has been no book so far in which it was fully discussed on the basis of reliable experimental data. In Chapter 3, the experimental results of the effect of the intermediate principal stress, which I obtained in the 1970s, are presented in a detailed manner, both in graphic and numerical forms. These results show the importance of the noticeable effect of the intermediate principal stress on the ultimate strength of rocks, that has been unjustifiably neglected or disregarded by Coulomb (1773), Mohr, Griffith and other strength theories which have been widely applied for a long time. They also show that the intermediate principal stress strongly influences the deformation and failure mode of rocks. On these experimental results, a new failure (fracture and yield) criterion is proposed. Furthermore, acoustic emission phenomena in rock under various stress states, and friction in rocks measured by a newly designed shear testing machine are discussed in relation to earthquake phenomena. Following on from these subjects, some noticeable features in the occurrence of recent large earthquakes are discussed.

Rock mechanics constitutes a branch of the material sciences. In the material sciences, the manufacturing of materials can be controlled in many cases. However, rocks are natural substances whose processes of generation and history of alteration in the Earth's crust are complex and generally unknown. In the early stages of the development of rock mechanics, numerous measurements in the laboratory were carried out without careful consideration of the complexity of rock materials. Therefore, for

example, the compressive strength values of rock specimens taken from rock masses fluctuate greatly. Such data may be useful for practical purposes. However, empirical formulae derived from them should be discriminated from natural formulae that have a certain physical meaning. In order to promote rock mechanics as a modern material science, precise and specific experimental approaches should be especially devised. When investigating the fundamental properties of rocks, it is of utmost importance to reduce the extrinsic fluctuation of data and to increase the reproducibility of experimental results. For this purpose, the selection of suitable uniform rock samples and the development of new devices for reliable experimental tests with high accuracy are essential.

On the other hand, many rock materials and rock masses have inhomogeneous and anisotropic structures. In this book some experimental results are presented that show how these intrinsic features influence and may control the deformation mode and failure of rocks.

As mentioned above, this volume deals only with selected topics from the field of experimental rock mechanics. Consequently, the references are also limited; Drs M. S. Paterson and T.-f. Wong systematically reviewed almost all the remaining branches of rock mechanics, and listed many references in their book (M. S. Paterson and T.-f. Wong: Experimental Rock Deformation – The Brittle Field, Springer, Berlin 2005). Their book is suitable for anyone interested in subjects that are not covered in my book.

I am very grateful to Professor Marek Kwaśniewski, Editor-in-Chief of this Geomechanics Research Series, for inviting me to write this book and for his great help in the preparation of the manuscript, and to his assistant Mr. Ireneusz Szutkowski for his contribution of redrawing and/or remastering figures for the book. I am also grateful to Professor James J. Mori, Kyoto University, who read the latter part of the manuscript and gave valuable comments including English corrections. Technical support for experimental works by Hiromine Mochizuki and Kansaku Igarashi in the Earthquake Research Institute, Tokyo University is greatly appreciated. Finally, special thanks go to my wife Tomoko for her tireless support during the long writing and editing process.

About the author

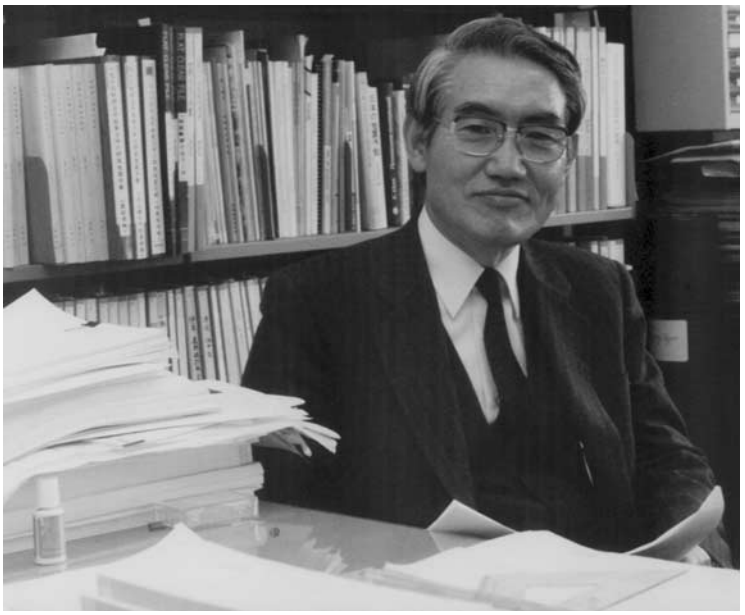

Intrigued by the postulation that earthquakes occur by sudden fracture in the earth's crust, Kiyoo Mogi devoted an important part of his professional career to Experimental Seismology. He has carried out laboratory studies of the fracture phenomena of rocks under stress to establish their relation to natural earthquakes. Advocating that important features of fractures and earthquakes depend largely on the degree of mechanical heterogeneity of rock, Professor Mogi has investigated various features of seismic activity, such as seismic gaps and migration phenomena. His development of the true triaxial compression machine, gave greater insight into the mechanical behaviour of the earth's materials by the use of systematic experiments. Using the data obtained from triaxial compression tests, a new, general failure criterion was proposed, also known as the "Mogi Failure Criterion", which could be referred to generation and development of earthquakes. The current book represents the results of 30 years of investigation by the author and his team of the mechanical behaviour of rocks. Besides this work and many prominent papers in international journals, Kiyoo Mogi also authored the book "Earthquake Prediction", 1985, published by Academic Press, Tokyo.

Kiyoo Mogi (1929, Yamagata, Japan) studied Geophysics at the University of Tokyo. After obtaining his Ph.D. degree in 1962, he was employed as a research associate and an associate professor at the Earthquake Research Institute of the University of Tokyo, before becoming a Professor of Experimental Seismology from 1969 to 1990. After this period, he was Professor in Earth Sciences at the Nihon University in Narashino City, near Tokyo, until the year 2000. Kiyoo Mogi has held the positions of President of the Seismological Society of Japan and Director of the Earthquake Research Institute of University of Tokyo. He has also been the Chairman of the Coordinating Committee for Earthquake Prediction, Japan (1991–2000) and of the Earthquake Assessment Committee for the "Tokai Earthquake", Japan (1991–1996). Kiyoo Mogi is currently Professor Emeritus at the University of Tokyo, and Fellow of American Geophysical Union.

SELECTED PUBLICATIONS

Mogi, K. (1956). Experimental study of diffraction of water surface waves. *Bull Earthq. Res. Inst., Univ. Tokyo*, **34**, 267–277.

Mogi, K. (1958). Relations between the eruptions of various volcanoes and the deformations of the ground surfaces around them. *Bull. Earthq. Res. Inst., Univ. Tokyo*, **36**, 99–134.

Mogi, K. (1962). Study of elastic shocks caused by the fracture of heterogeneous materials and its relation to earthquake phenomena. *Bull. Earthq. Res. Inst., Univ. Tokyo*, **40**, 125–173.

Mogi, K. (1963). Some discussions of aftershocks, foreshocks and earthquake swarms-the fracture of a semi-infinite body caused by inner stress origin and its relation to the earthquake phenomena (3). *Bull. Earthq. Res. Inst., Univ. Tokyo*, **41**, 615–658.

Mogi, K. (1967). Earthquakes and fractures. *Tectonophysics*, **5**, 35–55.

Mogi, K. (1968). Sequential occurrences of recent great earthquakes. *J. Phys. Earth*, **16**, 30–36.

Mogi, K. (1968). Source locations of elastic shocks in the fracturing process in rocks (1). *Bull. Earthq. Res. Inst., Univ. Tokyo*, **46**, 1103–1125.

Mogi, K. (1970). Recent horizontal deformation of the earth's crust and tectonic activity in Japan (1). *Bull. Earthq. Res. Inst., Univ. Tokyo*, **48**, 413–430.

Mogi, K. (1971). Fracture and flow of rocks under high triaxial compression. *J. Geophys. Res.* **76**, 1255–1269.

Mogi, K. (1972). Fracture and flow of rocks. In *The Upper Mantle*, A. R. Ritsema (ed.), *Tectonophysics*, **13**, 541–568.

Mogi, K. (1974). On the pressure dependence of strength of rocks and the Coulomb fracture criterion. *Tectonophysics*, **21**, 273–285.

Mogi, K. (1977). Dilatancy of rocks under general triaxial stress states with special reference to earthquake precursors. *J. Phys. Earth*, **25**, Suppl., S 203–S 217.

Mogi, K. (1981). Seismicity in western Japan and long term earthquake forecasting. In *Earthquake Prediction, an International Review. M. Ewing Ser. 4*, D. Simpson and P. Richards (ed.), Washington, D.C., Am. Geophys. Union, 43–51.

Mogi, K. and H. Mochizuki (1983). Observation of high frequency seismic waves by a hydrophone directly above the focal region of the 1980 earthquake (M6.7) off the east coast of the Izu Peninsula, Japan. *Earthquake Predict. Res.*, **2**, 127–148.

Mogi, K. (1985). Temporal variation of crustal deformation during the days preceding a thrust-type great earthquake — The 1944 Tonankai earthquake of magnitude 8.1, Japan. *Pageoph*, **122**, 765–780.

Mogi, K. (1985). *Earthquake Prediction*. Academic Press, Tokyo, 355pp.

Kwasniewski, M. and K. Mogi (1990). Effect of the intermediate principal stress on the failure of a foliated anisotropic rock. In *Mechanics of Jointed and Faulted Rock*, H-P. Rossmanith (ed.), Balkema, Rotterdam, 407–416.

Mogi, K. (2004). Deep seismic activities preceding the three large "shallow" earthquakes off south-east Hokkaido, Japan — the 2003 Tokachi-oki earthquake, the 1993 Kushiro-oki earthquake and the 1952 Tokachi-oki earthquake. *Earth Planets Space*, **56**, 353–357.

Mogi, K. (2004). Two grave issues concerning the expected Tokai Earthquake. *Earth Planets Space*, **56**, Ii–Ixvi.

I

Deformation and Fracture of Rocks

CHAPTER 1

Precise measurements of fracture strength of rocks under uniform compressive stress

The conventional compression test, in which a short, right cylinder is loaded axially, is one of the most widespread experimental procedures in rock mechanics. This configuration is used in studies of both brittle and ductile behavior, in long term creep studies as well as in studies of elastic behavior. In view of this wide usage, it is rather surprising to find so little concern with what are widely recognized as bad features of this test (Seldenrath and Gramberg, 1958; Fairhurst, 1961).

In the typical arrangement, for example, the steel of the testing machine contacts the rock cylinder, as shown in Fig. 1.1. Because steel and rock have different elastic properties, radial shearing forces are generated at the interface when load is applied to the rock sample. For most rocks these act inward and produce a *clamping effect* at the end of the cylinder (Filon, 1902). This causes two things to happen. First, because of the abrupt way in which the shearing stress changes near the outer edge of the steel-rock interface, a stress concentration arises (Nadai, 1924). Second, if a fracture propagates into the region near the end of the sample, growth of the fracture may be

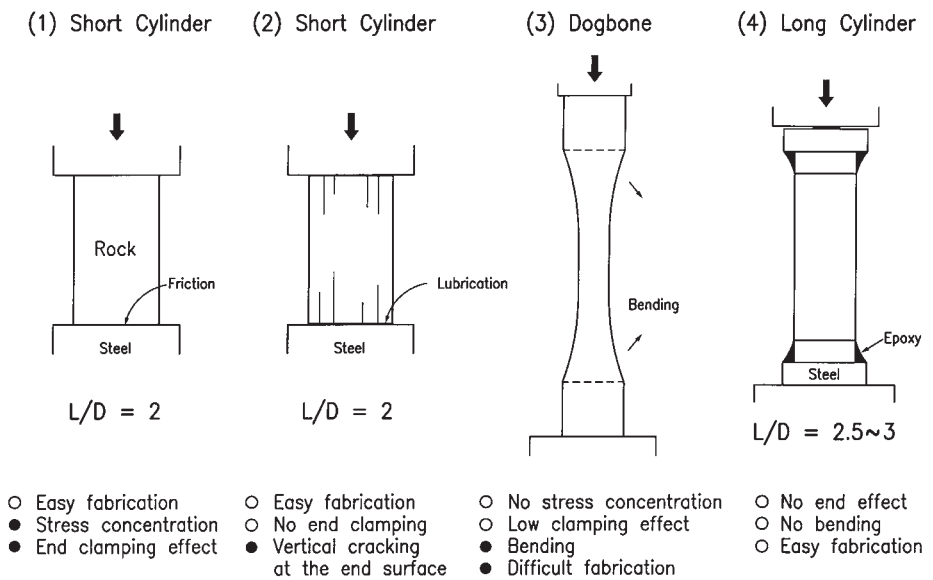

Figure 1.1. Various methods of testing rock samples under uniaxial compression conditions.

impeded. These two effects might influence the apparent strength of a typical rock differently: the stress concentration would tend to lower, while the clamping would tend to raise the apparent strength. Almost certainly, the effects do not cancel each other out.

One can think of a number of ways to eliminate these effects and thereby improve the compression test. As a simple method to eliminate the clamping end effect caused by friction on the steel-rock interface, various kinds of lubricants were applied between the rock end surface and the steel platen, as shown in Fig. 1.1 (2). In this case, a number of vertical cracks developed starting from the end surface of rock sample. This phenomenon seems to occur because of the intrusion of soft lubricator into the rock specimen. The compressive strength obtained by this method is different for different lubricants. Therefore, this method is not recommended.

Another simple method might be to make contact with the cylinder of rock through a metal which had identical mechanical properties. Then, no shearing forces would exist at the testing machine-rock interface, and, hence, there would be no stress concentration at the corners. However, faults might still be checked at the interface, for the typical short specimens that are used. The length/diameter ratio is usually around 2 so that any fault with a natural inclination of less that about 25° to the maximum compression would intercept one of the end faces. Actually, it is difficult if not impossible to match mechanical properties of rock with metals because most rocks exhibit complex non-elastic features prior to fracture. Therefore, this approach holds little promise.

Another approach is the improvement of sample shape, whereby the effect of a mismatch at the ends of the sample does not extend into the region of the sample where fracture occurs. One such design, suggested by Brace (1964), consists of a "dog-bone"-shaped specimen with a reduced central section and large radius as shown in Fig. 1.1 (3). According to three-dimensional photoelastic analysis (Hoek, personal communication to Brace), the stress concentration in the fillets of these specimens was extremely small and could be ignored. Of course, the stress concentration at the steel-rock interface and the associated clamping effect still existed in this specimen, but these had no effect on what happened in the central section, which, in Brace's design, had an area one fourth of that of the ends. Brace's specimens were quite slender so that bending stresses were present. Rather than go to extreme measures to eliminate them, they were simply evaluated by strain gages and the axial stresses corrected for bending in each experiments.

1.1 PRESENT SPECIMEN DESIGN

Brace's specimens have one drawback in that they require a grinding technique more elaborate than that used for producing straight cylinders. A new design was proposed by Mogi (1966) which combines the better features of Brace's specimen with greater ease of manufacture. The specimen (Fig. 1.2) is a long right cylinder connected to steel

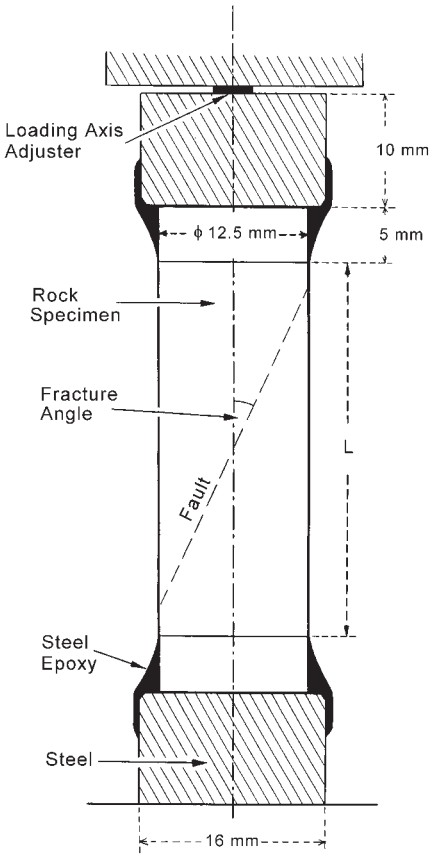

Figure 1.2. The recommended test specimen design.

end pieces by epoxy which is a commonly available commercial variety which contains a filler of fine steel particles. The thickness of the epoxy is gradually decreased from the steel end pieces toward the middle of the specimen to form a smooth fillet.

The gradual decrease of the thickness of epoxy probably eliminates most of the stress concentration at the contact of rock with steel. As the steel-filled epoxy has a modulus somewhat less than most rocks, the exact surface shape of the fillet is not critical. The absence of a stress concentration near the end of the specimen is shown by the way in which samples fractured. Fractures remained near the central section and did not enter the fillet region of the sample. No partially formed fractures could be found in the fillet region. Yoshikawa and Mogi (1990) showed by a numerical calculation that there is no stress concentration near the fillet region and the stress distribution is homogeneous in the main part, as shown in Fig. 7.23.

Although the stress concentration near the ends is removed, the end part may give a clamping effect. To avoid the influence of clamping, the specimen has a length which allows propagation of fractures completely within a uniform stress field. This critical length is discussed in more detail below.

With the longer sample required to avoid the clamping effect, bending becomes likely, due mainly to a mismatch of loading and specimen axes. Bending was kept to a minimum here by (a) keeping the ends of the sample accurately parallel, (b) by applying the load at a small central area of the upper steel piece (called "loading axis adjuster" in Fig. 1.2), and (c) by keeping the length of the end pieces as small as possible. This is also discussed below.

In summary, this sample design appears to be more practical than Brace's specimen, and it eliminates most of the bad features present in the conventional short cylinder. Yet, it is almost as easy to fabricate as the conventional specimen, as the rock part is still a circular cylinder. Application of the method to extension tests will be mentioned in Section 3.2.b.

1.2 EFFECT OF LENGTH/DIAMETER RATIO ON APPARENT STRENGTH AND FRACTURE ANGLE

As mentioned above, apparent strength in short specimens becomes higher due to the clamping effect. With the increase of the length/diameter ratio, this effect should decrease gradually and disappear at some critical value. Above this critical value, the strength should remain constant and should represent the true strength under uniform compression. To obtain this value and the critical length/diameter ratio, relations between apparent strength and length/diameter ratio were experimentally investigated for uniaxial and triaxial compression. In these experiments, the triaxial testing apparatus designed by Brace was used for uniaxial and triaxial compression tests. Strain rate was held constant at about 10^{-4} sec^{-1}.

The author carried out careful measurements of the apparent compressive strength and fracture angles of Dunham dolomite, Westerly granite and Mizuho trachyte as functions of the length/diameter ratio using the above-mentioned test specimens (Mogi, 1966). Dunham dolomite and Westerly granite are compact and uniform in structure, while Mizuho trachyte is rather porous (porosity 8.5%) with a non-uniform distribution of pores. The results are summarized in Table 1.1 and Figs 1.3, 1.4 and 1.5. Here, L and D are length and diameter of the central cylindrical part of specimen, respectively.

Dunham dolomite (Fig. 1.3). The average values of two or three strength measurements and the standard deviation are indicated in the figure. The reproducibility of strength (1 per cent or better) is very good. This is probably due to the homogeneous structure of this rock and the high accuracy of the present measurement. The apparent strength decreases markedly with the increase of L/D, but the value becomes nearly constant at high values of L/D. The critical value, (L/D)c, above which the apparent strength becomes nearly constant is about 2.5. In this rock, the fracture is of the typical shear type. The angle between the fracture and the loading axis also decreases markedly with increase of L/D and becomes nearly constant (20°) above (L/D)c. In Fig. 1.3 (lower), large closed circles indicate angles of fault planes which go through

Table 1.1. Apparent strength of specimens with different length/diameter ratio under uniaxial compression.

Rock	*L*/*D*	No. of Specimens	Apparent strength, MPa	Relative strength, %
Dunham dolomite	1.25	2	232 ± 1	111.5
	1.50	3	225 ± 3	107.5
	1.75	2	224 ± 3	107
	2.00	3	219 ± 3	104.5
	2.25	2	214 ± 0	102.5
	2.50	2	209 ± 0	100
	3.00	2	208 ± 0	99.5
	4.00	1	207	99
Westerly granite	1.25	2	263 ± 9	109.5
	1.50	2	252 ± 2	105
	1.75	2	248 ± 2	103.5
	2.00	3	247 ± 5	102.5
	2.25	3	242 ± 4	100.5
	2.50	4	240 ± 6	100
	3.00	2	239 ± 4	99.5
	3.50	2	238 ± 6	99
	4.00	3	238 ± 5	99
Mizuho trachyte	1.00	1	126	115.5
	1.50	1	114	104.5
	1.75	1	112	103
	2.00	1	110	101
	2.25	1	112	102.5
	2.50	1	110	100
	3.00	1	109	99.5

the whole sample and small closed circles indicate partial fault planes. In addition to actual faults, regular patterns of microfractures with no shear displacement were observed in the central part of certain specimens. The angle between these microfractures and the loading axis is indicated by open circles. Clearly, the orientation of the main faults depends on L/D, whereas the orientation of microfractures does not. Also, the former coincides with the latter for large L/D values. The dotted curve (1) in Fig. 1.3 (lower) gives a calculated value of θ from

$$\cot\theta = \mathrm{L/D} \tag{1.1}$$

where θ is an apparent fracture angle. Curve (2) is calculated from

$$\cot\theta = (\mathrm{L} + 0.25)/\mathrm{D} \tag{1.2}$$

and takes into account the actual intersection that a straight fault would have some 3 mm above the base of the fillet, rather than exactly at the base of the fillet as in (1).

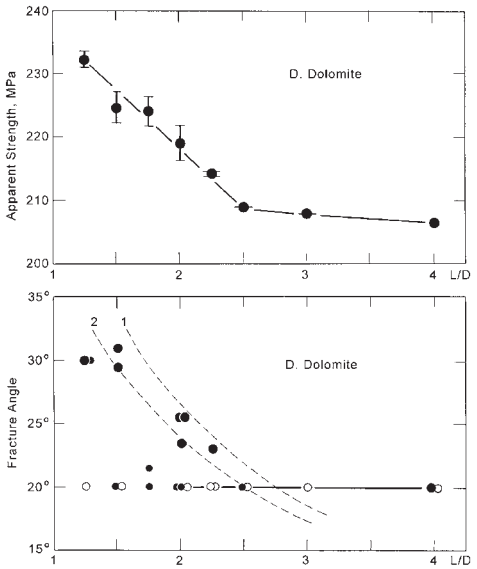

Figure 1.3. Relations of apparent compressive strength (top figure) and apparent fracture angle (bottom figure) to length/diameter ratio in Dunham dolomite. In the bottom figure, large closed circle: good fault; small closed circle: partial fault; open circle: microfractures; dotted lines 1 and 2: calculated curves.

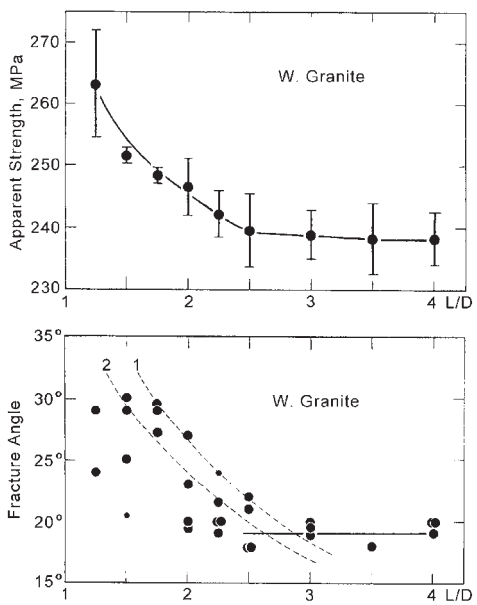

Figure 1.4. Relations of apparent uniaxial compressive strength (top figure) and apparent fracture angle (bottom figure) to length/diameter ratio in Westerly granite.

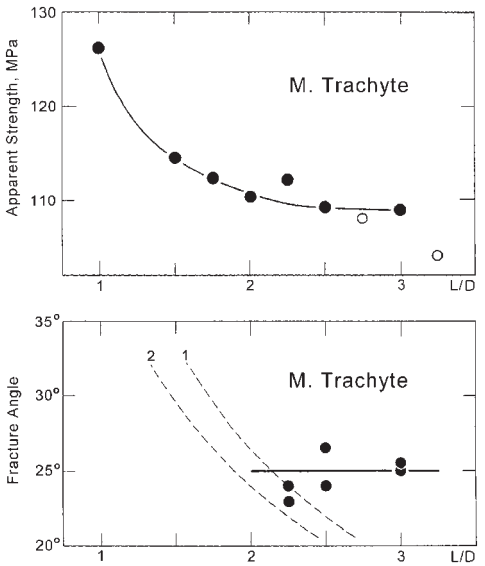

Figure 1.5. Relation of apparent uniaxial compressive strength (top figure) and apparent fracture angle (bottom figure) to length/diameter ratio in Mizuho trachyte. Open circle: accompanied by bending.

The observed points are seen to lie somewhat between curves (1) and (2), which suggests that the fault angle in short specimens is strongly effected by clamping at the ends of the specimens. That is, the fault is forced to run between opposite corners of the sample.

Westerly granite (Fig. 1.4). The effect of L/D on strength and fracture angle is very similar to that in dolomite, except for a greater fluctuation of strength values. This fluctuation (less than 3%) may be due to the larger grain size and high brittleness of this rock. The apparent strength becomes constant in longer specimens. The critical value of L/D is also 2.5. Apparent fracture angles also change with L/D and become constant (19°) in longer specimens. In this case, the typical fracture surface was not so flat as in the dolomite and no microfractures were observed.

Mizuho trachyte (Fig. 1.5). The apparent strength also decreases with the increase of L/D and becomes constant above a critical value (2.0) of L/D, but this value is smaller than those obtained for the above-mentioned dolomite and granite. The final value of the fracture angle is larger (25°) than the other two. In this rock, a bending fracture was sometimes produced at higher values of L/D; such a fracture forms perpendicular to the specimen axis. The apparent strength of the other two was considerably lower than the normal case, as indicated by open circles in Fig. 1.5 (upper). The bending may have been caused by an uneven stress distribution in the specimen due to the porous structure.

Thus, the effect of L/D on apparent strength and fracture angle for these three rocks is important in shorter specimens. Above a critical value of L/D, strength and

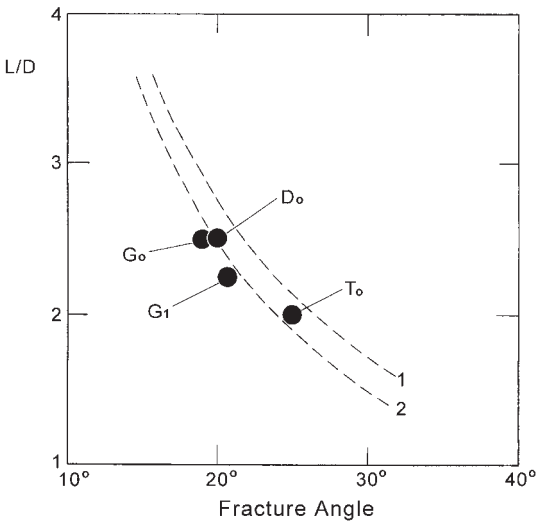

Figure 1.6. Relation between fracture angle and the critical length/diameter ratio above which the end fix effect disappears. Broken lines 1 and 2: calculated curves; D_0: dolomite (confining pressure = 0.1 MPa); G_0: granite (0.1 MPa); G_1: granite (17 MPa); T_0: trachyte (0.1 MPa).

fracture angle were independent of L/D. This final value of strength and fracture angle probably represents the strength and fracture angle under uniform compressive stress for the following reasons: (1) The fracture starts and ends inside the central part of specimen. Therefore, stress concentrations at the end have no effects on strength. (2) Strength and fracture angle are independent of L/D, so the clamping effect is also avoided. (3) If bending is important, apparent strength should decrease with increase of the length of specimen. Here, since such a strength decrease is small in longer specimens ($L/D < 4$), so that bending effect is probably not significant.

The relation between the critical length/diameter ratio (L/D)c and the final fracture angle θ_0 is presented in Fig. 1.6. Curves (1) and (2) in this figure are calculated as given above. The agreement between the observation and the calculation is good, especially for curve (2).

A number of researchers have investigated the effect of length/diameter ratio on apparent uniaxial compressive strength for rocks (e.g., Obert et al., 1946; Dreyer et al., 1961) and for concrete (e.g., Gonnerman, 1925; Johnson, 1943; A.C.I., 1914). These previous experiments were carried out employing the conventional method in which straight circular cylinders or prisms were used, and therefore stress concentrations at the end of specimen were probably present. In Fig. 1.7, some results of these previous experiments (bottom figure) are presented together with the above-mentioned results (top figure). The apparent strength considerably decreases with the increase of length/diameter ratio (L/D). The strong effect of L/D in shorter specimens ($L/D < 2$) is clearly caused by the clamping effect. And these previous experiments did not give a constant final value of strength and fracture angle for large L/D. Apparent strength

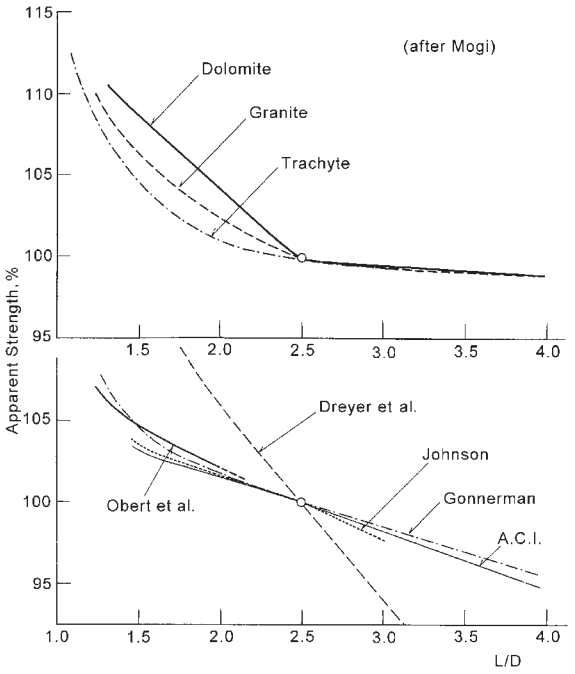

Figure 1.7. Comparison of the author's results (Mogi, 1966) (top figure) with some previous experiments (bottom figure). The relative strength is recalculated for strength at $L/D = 2.5$. Obert et al. (1946): average for various rock types; Dreyer et al. (1961): rock salt; A.C.I. (1914), Gonnerman (1925), Johnson (1943): concrete.

still continues to decrease with L/D above the expected critical length/diameter ratio. This could have been due to bending caused by a mismatch of specimen and loading axis, or by the non-uniform structure of rock and concrete.

One example in the previous reports on similar measurements on an andesite by Shimomura and Takata (1961) is presented in the left figure of Fig. 1.8. The fluctuation of strength values (~50%) in their experiment is much greater than that of the above-mentioned Dunham dolomite shown in the right figure. From this experimental result, it is impossible to obtain any significant information. Such great fluctuation may be due mainly to high inhomogeneity of the rock samples. These previous experimental results presented in Fig. 1.7 and Fig. 1.8 show that a suitable selection of mechanically uniform rock samples is very important in rock mechanics.

1.3 COMPARISON WITH THE CONVENTIONAL METHOD

As mentioned above, the conventional test, which uses short cylinders, is accompanied by stress concentration and the clamping effect. Specimens of length/diameter ratio 2 were used in most previous experiments. According to the present results, such tests

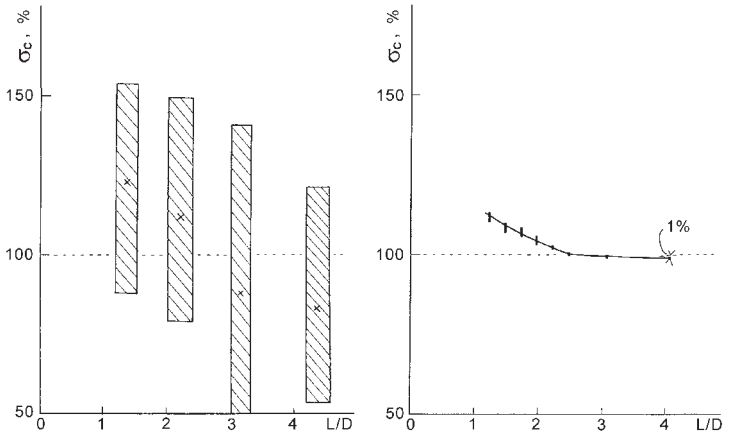

Figure 1.8. Simplified relations of apparent strength (relative values) to length/diameter ratio. Left figure: andesite (Shimomura and Takata, 1961); right figure: Dunham dolomite (Mogi, 1966).

may give considerably higher strength and larger fracture angle. Furthermore, since the end parts of the cylinder are laterally fixed to a hard end piece, the length of the central part where the stress is nearly uniform is still shorter than the actual length. For comparison with the present method, some uniaxial compression tests were carried out using the conventional method. In Dunham dolomite, the strength measured was 231 MPa and the fracture angle was 30°. These values are 10 per cent and 50 per cent higher, respectively, than those obtained using the present method. For Westerly granite, strength and fracture angle were 250 MPa and 26°. These are 5 per cent and 36 per cent higher than those obtained using the present method. Thus, applying the conventional test to such hard rocks may give considerably higher strength and larger fracture angle. In Mizuho trachyte, for which the true fracture angle is higher, the difference between the revised method and the conventional method was not appreciable.

Thus, the precise measurements of true compressive strength and fracture angle under uniaxial compression can be best carried out by use of the revised specimen design which is a longer cylinder with a smooth epoxy fillet at the end of rock specimen, as shown in Fig. 1.1 (4). And it should be noted that the length/diameter ratio should be larger than 2.5.

1.4 DECREASE OF THE END EFFECTS BY CONFINING PRESSURE

It was expected that end effects might change with confining pressure. To investigate this, apparent strength and fracture angle of the specimens having various length/diameter ratio were measured under confining pressure (Mogi, 1966). The shape of specimen and the experimental procedure are similar to the case of uniaxial

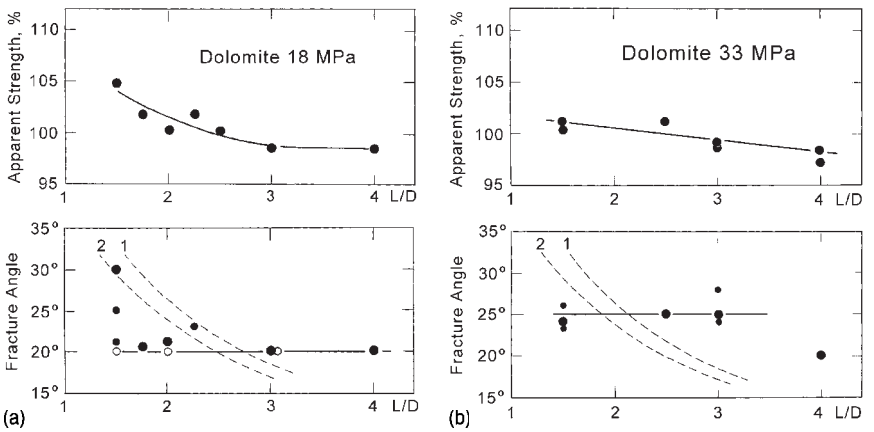

Figure 1.9. Relation of apparent strength (top figure) and apparent fracture angle (bottom figure) to length/diameter ratio in Dunham dolomite under confining pressure of 18 MPa (a) and 33 MPa (b).

compression, except for jacketing of the specimen to prevent the intrusion of pressed oil. Corrections were made for the frictional force between the axial piston and the o-ring seal of the pressure vessel. (The experiments under confining pressure are discussed in detail in the following chapter.)

Dunham dolomite. The results are presented in Figs. 1.9 (a) and 1.9 (b). Under 18 MPa confining pressure, the final fracture angle and the critical value of L/D are nearly the same as in the uniaxial case. However, the effect of L/D on strength is considerably smaller than in the uniaxial case. Strength and fracture angle under 33 MPa confining pressure is nearly independent of L/D.

Westerly granite. The effect of L/D was determined at a confining pressure of 17 MPa, 51 MPa, and 108 MPa. With the increase of pressure, the effect of L/D on strength and fracture angle decreases, as shown in Figs. 1.10 (a)–1.10 (c). The fracture angle gradually increases with confining pressure and the critical value of L/D also decreases.

Thus, it is concluded that end effects decrease gradually with an increase of pressure and become very small under confining pressure greater than 30–50 MPa, as shown in Fig. 1.11. This decrease of end effect may be due to (1) the relative decrease of the effect of lateral restriction at the end part by increase of lateral pressure, (2) the increase of fracture angle under pressure, and (3) the increase in the ductility of rocks. The observations show that the shape of the specimen becomes less critical at high pressure and so the conventional triaxial compression test may also give as nearly correct results as the method used here.

This discovery of the marked decrease of the end effect by confining pressure provided *a key for the design of the true triaxial compression machine* (Mogi, 1970), which is explained in Chapter 3.

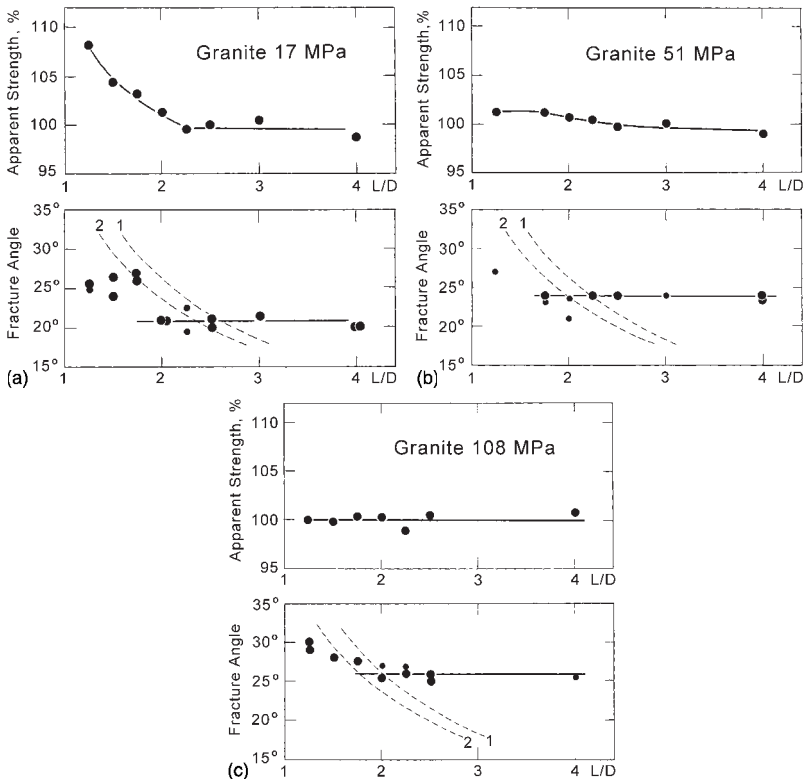

Figure 1.10. Relation of apparent strength (top figure) and apparent fracture angle (bottom figure) to length/diameter ratio in Westerly granite under confining pressure of 17 MPa (a), 51 MPa (b) and 108 MPa (c).

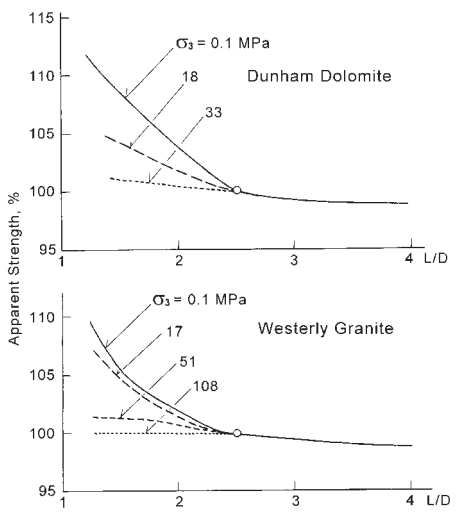

Figure 1.11. Relation of apparent strength to length/diameter ratio in Dunham dolomite (top figure) and Westerly granite (bottom figure).

REFERENCES

Am. Concrete Inst. (A.C.I.) (1914). Report of committee on specifications and methods of tests for concrete materials. Proc. Am. Concrete Inst., v. **10**, p.422.

Brace, W. F. (1964). Brittle fracture of rocks. In: State of stress in the Earth's Crust. Judd, W.R. (ed.) New York: Elsevier, 111–174.

Dreyer, W. and H. Borchert. (1961). Zur Druckfestigkeit von Salzgesteinen. Kali und Steinsalz, Heft **7**, S.234–241.

Fairhurst, C. (1961). Laboratory measurement of some physical properties of rock. In 4th Symp. on Rock Mechanics, Bull. Mineral Industries Expt. Sta. Penn. State Univ., No. 76. Hartman, H. L. (ed.), 105–118.

Filon, L. N. G. (1902). On the elastic equilibrium of circular cylinders under certain practical systems of load. Phil. Trans. R. Soc., London, Ser. A **198**, 147–233.

Gonnerman, H. F. (1925). Effect of size and shape of test specimen on compressive strength of concrete. Proc. A. S. T. M., v. **25** (Part 2), p.237.

Johnson, J. W. (1943). Effect of height of test specimen on compressive strength of concrete. A. S. T. M. Bulletin, No. 120, p.19.

Mogi, K. (1966). Some precise measurements of fracture strength of rocks under uniform compressive stress. Felsmechanik und Ingenieurgeologie **4**, 41–55.

Nadai, A. (1924). Über die Gleitund Verzweigungsflächen einiger Gleichgewichtszustände, Z. Physik 30, p.106.

Obert, L., S.L. Windes and W. I. Duvall. (1946). Standardized tests for determining the physical properties of mines rocks. U. S. Bur. Mines. Rep. Invest., no. 3891, p.1.

Seldenrath, Th. R. and J. Gramberg. (1958). Stress-strain relations and breakage of rocks. In: Mechanical Properties of Non-Metallic Materials. Walton, W. H. (ed.). London: Butterworths, 79–102.

Shimomura, Y. and A. Takata. (1961). On the mechanical behaviors and the breaking mechanism of rocks (1st Report) — Shape and scale effect on fracture of rock specimens in compression. J. Mining and Metallurgical Inst. of Japan, Vol. **77**, No. 876, 9–14. (in Japanese)

Yoshikawa, S. and K. Mogi. (1990). Experimental studies on the effect of stress history of acoustic emission activity – A possibility for estimation of rock stress. J. Acoustic Emission, *8*, 113–123.

CHAPTER 2

Deformation and failure of rocks under confining pressure

A state of stress that is necessary to produce rock failure in an element can be described by the three principal stresses σ_1, σ_2, and σ_3. In this book, compressive stress is taken positive and $\sigma_1 > \sigma_2 > \sigma_3$, that is, σ_1 is the maximum principal stress, σ_2 is the intermediate principal stress, and σ_3 is the minimum principal stress. In principal coordinates, the points $(\sigma_1, \sigma_2, \sigma_3)$ representing different states of stress necessary to produce failure might form a surface

$$\sigma_1 = \mathrm{f}(\sigma_2, \sigma_3) \tag{2.1}$$

for a given material. The most fundamental problem of rock mechanics is the study of the shape of this surface for various rocks. In the next chapter, this is fully discussed.

Many experiments have been done using the so-called triaxial test, in which two principal stresses are equal, $\sigma_1 > \sigma_2 = \sigma_3 > 0$ (e.g., von Kármán, 1911; Griggs, 1936; Handin, 1966) or $\sigma_1 = \sigma_2 > \sigma_3 > 0$ (e.g., Böker, 1915). In this book, the term "conventional triaxial test" is used for such cases, and the true triaxial test is used for the general case in which $\sigma_1 \geq \sigma_2 \geq \sigma_3$. In this chapter, deformation characteristics and pressure dependence of rock strength by the conventional triaxial compression test are discussed, mainly on the basis of the author's experiments.

2.1 DEFORMATION CHARACTERISTICS

2.1.a *Experimental procedure*

First, rock specimens of various types from Japan were tested at room temperature by the conventional triaxial compression method (Mogi, 1965). The testing apparatus at Waseda University in Tokyo was used in the experiments. The schematic view of the apparatus is presented in Fig. 2.1. The test specimens were cylinders of 40 mm diameter for weaker rocks and 20 mm diameter for hard rocks, the height/diameter ratio being nearly 2.0. In this case, there is the end effect for hard rocks under low confining pressure, but the revised specimen design described in the preceding chapter was used for Westerly granite and Dunham dolomite which will be discussed later in this chapter. The specimens were jacketed with soft rubber to prevent pressure fluid from entering porous rock specimens. (Thereafter, I frequently used silicone rubber for jacketing.) The axial stress was applied by a hydraulic testing machine. The confining pressure was supplied independently by another oil compressor. The value of confining pressure was measured by a Bourdon gage. The axial load was

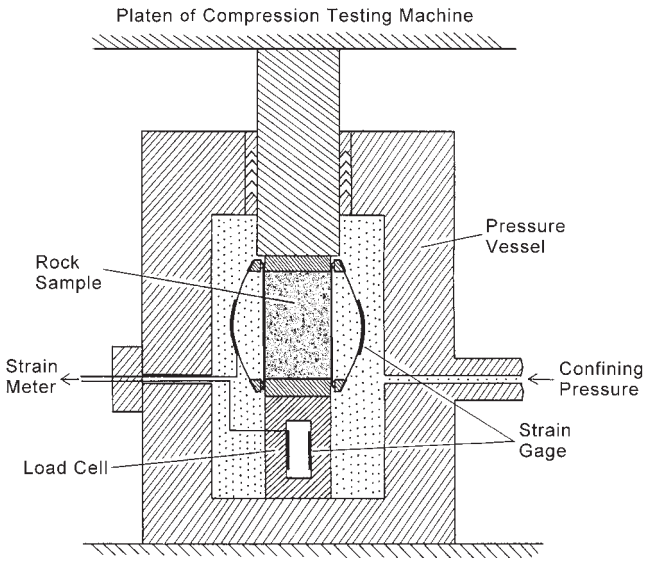

Figure 2.1. Schematic view of the triaxial apparatus.

measured by a load cell situated between a steel end piece fixed to the test specimen and the bottom of the pressure vessel. The load cell, a closed hollow steel cylinder with an electric resistance strain gage bonded to the inside of the cylinder, measured the axial load without any frictional error.

In Fig. 2.2, various methods of the axial strain measurement are shown. The external method (1) in this figure, using a dial gage or differential transformer in which the strain is obtained from the displacement of the piston of the press, is not accurate enough for a precise analysis of the stress-strain curve and it is not applicable for cyclic loading because this system shows a remarkable hysteresis. For precise measurements of strain, the internal method (2) of which the two methods (a) and (b) are schematically shown in Fig. 2.2. In the first method (a), the electric resistance strain gage is bonded directly onto the surface of the rock specimen. This method is highly sensitive and easy-to-use, therefore it is used most often. However, method (a) is unsuitable to measure the mean strain in heterogeneous deformation including microcracks, small faults, etc. and to measure large deformation. In method (b), bending steel plates are fixed to the upper and lower steel end pieces connected to the rock specimen, and shortening of the rock cylinder causes the bending of the thin steel plates. The bending deformation of the plate is measured by the bonded strain gages. As the elastic distortion of steel end pieces is generally negligible because of its slight thickness, the strain gage output indicates the axial strain of the rock specimen. Since this system of strain measurement does not show any appreciable hysteresis for loading and unloading, this method is applicable for cyclic loading experiments, and also is suitable for large deformation measurements.

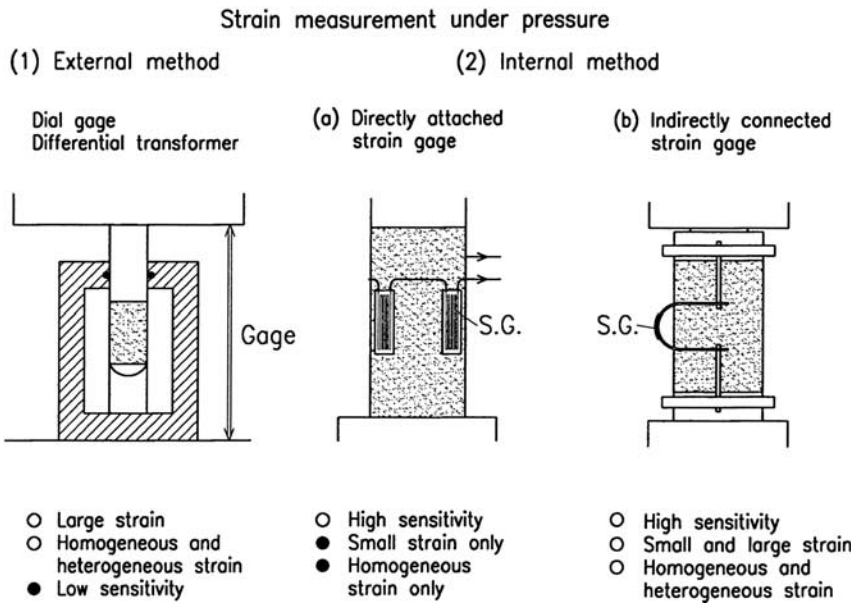

Figure 2.2. Various methods of the axial strain measurement.

However, the behavior of electric resistance type strain gage should be examined under confining pressure, because there was a question that the strain gage might show an appreciable "pressure effect" due to hydrostatic pressure. To examine this "pressure effect", the change in strain measured by the electric resistance strain gage under confining pressure was compared with that in the atmospheric pressure, as shown in Fig. 2.3. Strains (A) and (B) are the axial strains of, respectively, the outside and the inside of the hollow steel cylinder with closed ends under axial compression. Open circles in Fig. 2.3 are in atmospheric pressure (0.1 MPa) and closed circles are in 130 MPa confining pressure. Since the relation between strain (A) and strain (B) is almost similar in both cases, the hydrostatic pressure does not give any significant effect to the gage factor.

Thus, method (b) shown in Fig. 2.2 or Fig. 2.1 is applicable to precise measurements of small and large strains of various rocks under cyclic loadings. The axial load was applied at a nearly constant strain rate of 0.15–0.2 percent per min. The differential stress was reduced to zero at various stages of deformation, the elastic and permanent strains were observed at each stage.

2.1.b *Stress-strain relation*

The rocks tested were a peridotite, a diorite, a granite (strength only), two andesites, a trachyte, three tuffs and a marble. The density and porosity of these rocks are shown in Table 2.1.

The test specimens were compressed to fracture for hard rocks and to 3–4 percent strain for soft rocks, and at various stages of deformation the stress was reduced to

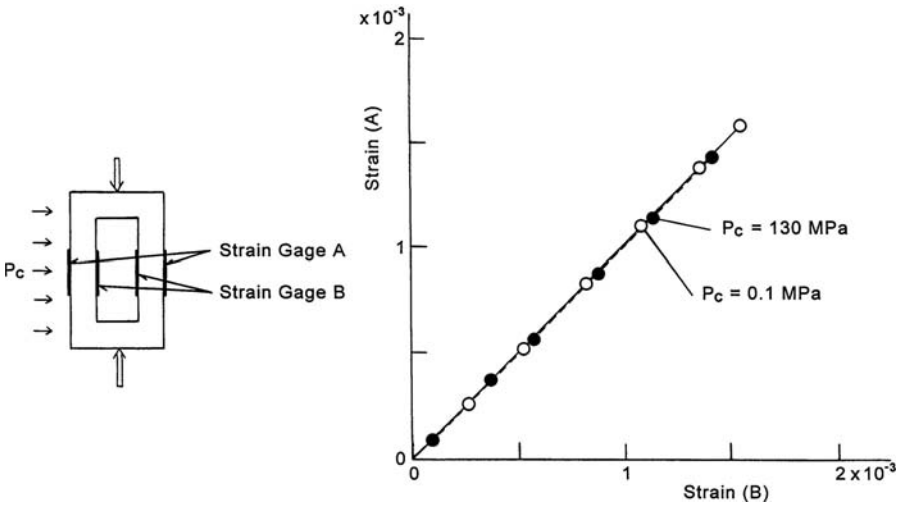

Figure 2.3. Strains (A) and (B) are the axial strains at, respectively, the outer and inner surface of the steel hollow cylinder with closed ends subjected to confining pressure.

Table 2.1. Tested rocks.

No.	Rock	Bulk density (g/cm^3)	Porosity (%)
1.	Nabe-ishi peridotite	3.16	0.02
2.	Orikabe diorite	2.78	0.4
3.	Mannari granite	2.62	0.7
4.	Mito marble	2.69	0.2
5.	Shirochoba andesite	2.45	5.1
6.	Tatsuyama tuff	2.26	10.2
7.	Mizuho trachyte	2.24	8.5
8.	Shinkomatsu andesite	2.17	12.6
9.	Ao-ishi tuff	2.01	17.3
10.	Saku-ishi welded tuff	1.95	21.6

zero or to very small values, then increased again. Stress-strain curves of some of these rocks under the conventional triaxial compression for different values of the confining pressure ($\sigma_2 = \sigma_3$) are shown in Figs. 2.4(a)–2.4(f). The vertical axis is the differential stress ($\sigma_1 - \sigma_3$) in MPa and the horizontal axis is the strain in percent.

The experimental results show that compact igneous rocks are very brittle and become markedly stronger with the increase of confining pressure, while other porous soft rocks become ductile even under low confining pressure. However, the precise feature of these curves suggests complex processes of deformation. For example, the initial part of deformation before yielding, the so-called *elastic part*, is significantly curved and includes appreciable permanent deformation in many cases. The simple

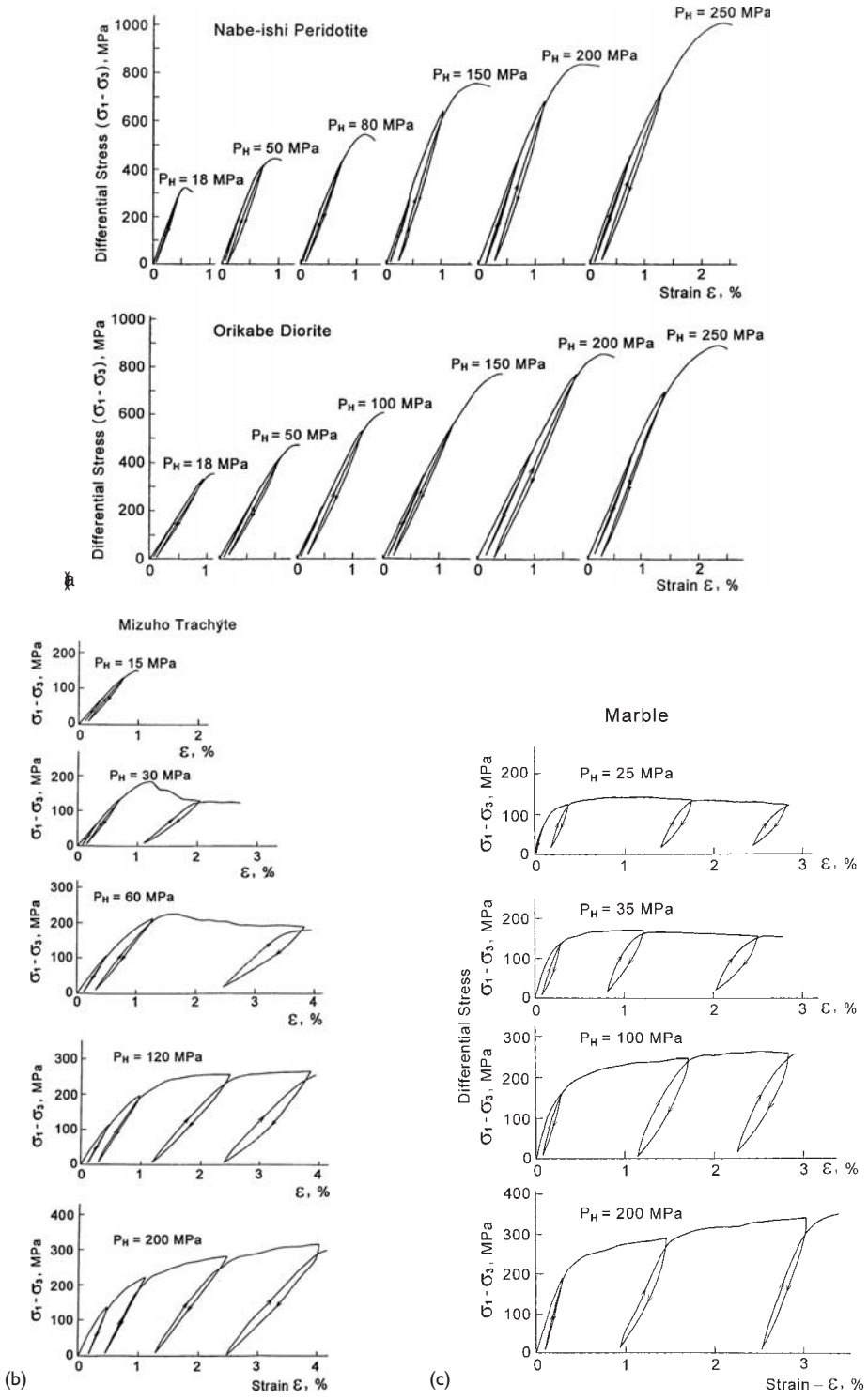

Figure 2.4(a)–(f). Stress-strain curves under cyclic axial loading of various kinds of rocks. P_H: confining pressure.